

Predicting the optimum compositions of highperformance Cu–Zn alloys via machine learning

Baobin Xie¹, Qihong Fang^{1,a)}, Jia Li^{1,b)}, Peter K. Liaw²

Received: 25 June 2020; accepted: 2 September 2020

In the alloy materials, their mechanical properties mightly rely on the compositions and concentrations of chemical elements. Therefore, looking for the optimum elemental concentration and composition is still a critical issue to design high-performance alloy materials. Traditional alloy designing method *via* "trial and error" or domain experts' experiences is barely possible to solve the issue. Here, we propose a "composition-oriented" method combined machine learning to design the Cu–Zn alloys with the high strengths, high ductility, and low friction coefficient. The method of separate training for each attribute label is used to study the effects of elemental concentrations on the mechanical properties of Cu–Zn alloys. Moreover, the elemental concentrations of new Cu–Zn alloys with the good mechanical properties are predicted by machine learning. The current results reveal the vital importance of the "composition-oriented" design method *via* machine learning for the development of high-performance alloys in a broad range of elemental compositions.

Introduction

Copper alloys are the foundation of the synchronous ring of automobile transmission. However, the traditional wearresistant Cu alloys, such as Cu-Sn and Cu-Al alloys, are hardly used in the rapid development of synchronous rings due to the low strengths, ductility, and wear resistance [1, 2, 3, 4, 5]. To improve the mechanical properties of traditional wear-resistant Cu alloys, one or more alloy elements, such as Ti, Co, P, Mg, Al, Sn, Mn, and Fe, can be introduced in a considerable amount of experimental work [6, 7, 8]. However, using the classical physics-based models to study the relationship between composition and mechanical property of the Cu alloys, it is easy to fall into the "dimension disaster" due to the complexity of the elemental compositions, which leads to a decrease in prediction accuracy of the classical physics-based models. Therefore, traditional composition design of the Cu alloys mainly depends on the "trial and error" method or the intuitive technique [9, 10, 11]. Now, the ability to find new materials through machine learning makes it possible for engineers to enhance the performance of existing materials [12, 13, 14].

As the most advanced computer technology, machine learning can deeply mine the internal relationship between data rather than rely on the inherent theoretical formula or experience, so that it can capture the highly-complex nonlinear input/output relationships. Furthermore, machine learning can traverse the predicted values in the global scope to quickly find the optimal value, which is crucial for material design. Recently, machine learning has been widely used in the field of materials science [14, 15, 16, 17, 18, 19]. The backpropagation artificial neural network (ANN) combined with a genetic algorithm is used to establish the inference model of the mechanical properties of low-alloy steels by the composition and heat treatment conditions [20]. Using this machine learning model, the effects of compositions and heat treatment conditions on the mechanical properties of low-alloy steels are revealed. In addition, the yield strength, ultimate strength, and elongation of the Cu-Sn-Pb-Zn-Ni alloy system can be predicted via machine learning [21]. By inputting alloy compositions and process conditions, the machine learning models can estimate the properties of alloys. Importantly, the relationship between composition and property obtained via machine learning can guide the selection of the potential alloys rapidly and accurately.

In the current study, we propose a "composition-oriented" design method for high-performance wear-resistant Cu–Zn alloys *via* machine learning. We use the multi-layer feed-



¹State Key Laboratory of Advanced Design and Manufacturing for Vehicle Body, Hunan University, Changsha 410082, PR China

²Department of Materials Science and Engineering, The University of Tennessee, Knoxville, Tennessee 37996, USA

^{a)}Address all correspondence to these authors. e-mail: fangqh1327@hnu.edu.cn

b)e-mail: lijia123@hnu.edu.cn



forward ANN algorithm to train three attribute labels of the original data set separately. Then, the trained models are used to study the effects of elemental concentrations on the mechanical properties of Cu–Zn alloys. According to the comparison of the comprehensive properties, the optimum range of elemental concentrations in Cu–Zn alloys can be found. Moreover, the new Cu–Zn alloys with the optimum elemental concentration predicted by machine learning have better mechanical properties.

Results and Discussion

Downloaded from https://www.cambridge.org/core. University of Tennessee Libraries, on 01 Jul 2021 at 04:17:48, subject to the Cambridge Core terms of use, available at https://www.cambridge.org/core/terms. https://doi.org/10.1557/jmr.2002.258

Figures 1(a)–1(c) plot the composition-UTS model, composition-EL model, and composition-FC model, respectively. Each figure contains the prediction results of a training set, testing set, and all data. The data points fall along the dotted line, indicating that the predicted value is consistent with the experiment [22]. We further linearly fit the predicted value with the experimental value. The fitting solid line is closer to the dotted line, revealing the higher accuracy predicted by the MLFFANN model. For the stage of training, Figs. 1(d)–1(f) show the loss evolution of composition-UTS model, composition-EL model, and composition-FC model, respectively. It can be seen that three MLFFANN models perform relatively well for the training set, testing set, and all data.

The predicted accuracy of the MLFFANN models is further validated, compared with the experimental data, which are not in original database (Table 1). These data is randomly selected from the experimental work [22] but does not participate in

training. In other words, they can represent the prediction ability of MLFFANN models for Cu–Zn alloys with random composition at the same process. Table 1 indicates that MLFFANN models accurately predict UTS, EL, and FC in Cu–Zn alloys. From Table 1, the prediction results of UTS and EL are better than those of FC. The main factors to determine UTS and EL of Cu–Zn alloys mainly depend upon the elemental concentration and composition [22]. The factors of FC rely on not only the composition and concentration but also the surface morphology [22].

According to the previous experimental results [22], the strengthening mechanism is mainly caused by different elemental concentrations in alloys [23, 24, 25, 26]. The strengthening mechanism of Cu alloys can be divided into (i) precipitation strengthening represented by Ni, Co, and Si; (ii) fine-grained strengthening represented by P; and (iii) solution strengthening represented by Mn. The yield strength based on the classical physical model can be expressed as follows [27]:

$$\sigma_{\rm Y} = \sigma_{\rm SS} + \sigma_{\rm GB} + \sigma_{\rm P},\tag{1}$$

where σ_Y represents yielding strength and σ_{SS} , σ_{GB} , and σ_P denote solution strengthening, fine-grained strengthening, and precipitation strengthening, respectively. Therefore, we use MLFFANN models to obtain the best elemental compositions and concentrations instead of classical physical models which consider the coupling effect of precipitate strengthening, fine-grain strengthening, and solution strengthening [25, 26, 27, 28, 29]. In addition, the MLFFANN model also avoids

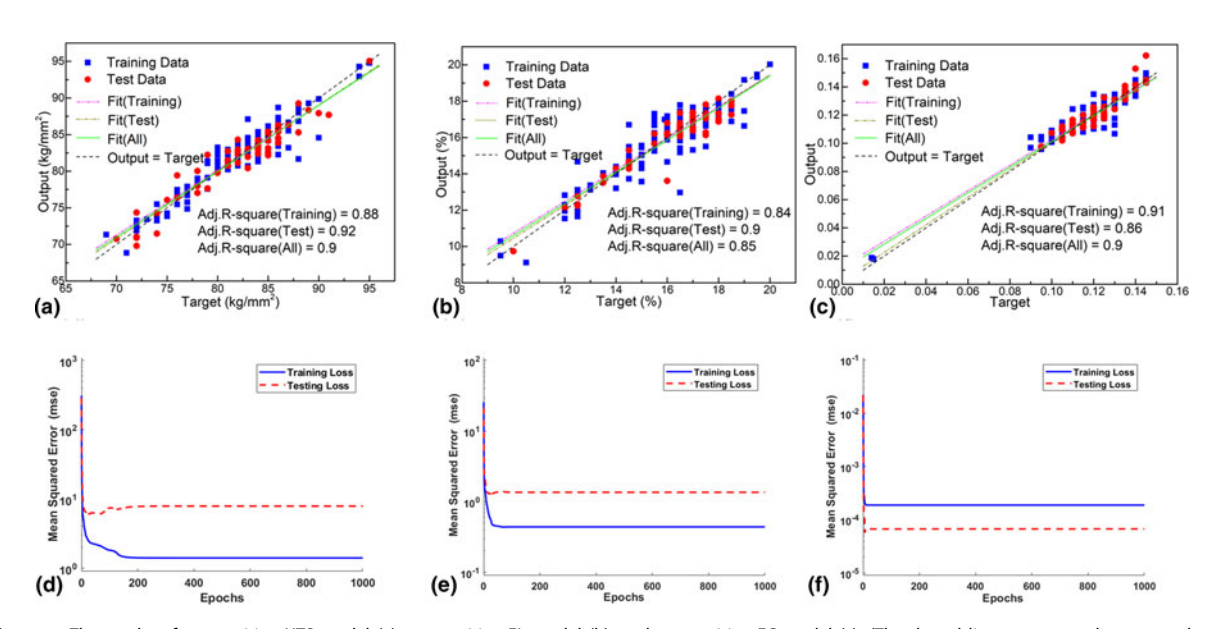


Figure 1: The results of composition-UTS model (a), composition-EL model (b), and composition-FC model (c). (The dotted line represents the output data in exactly the same as the target data in the all data set; the double-dash-dotted line means the regression result between the output data and the target data in the testing data set; the dash-dotted line refers the regression result between the output data and the target data in the training data set; the solid line represents the regression result between the output data and the target data in the all data set.) The loss evolution of composition-UTS model (d), composition-EL model (e), and composition-FC model (f).



TABLE 1: Validating data outside the original data set.

	Experim	ental results			Predicted resu	Error (%)			
Sample [21]	UTS	EL	FC	UTS	EL	FC	UTS	EL	FC
Cu-29.1Zn-10.8Al-1.79Ti	94	10	0.125	94.3	9.74	0.123	0.3	2.6	1.6
Cu-39.7Zn-5.1Al-1.75Ti	89	15	0.12	89.3	15.4	0.119	0.3	2.7	0.86
Cu-29.5Zn-4.8Al-0.11Zr-0.12P	85	16.5	0.09	82.6	16.6	0.096	2.8	0.6	6.7
Cu-28.6Zn-5Al-0.18Zr-0.03Co-0.058Sn	83	17.5	0.095	82.5	17.04	0.107	0.6	2.6	12.6
Cu-29.1Zn-4.9Al-0.11Ti	86	17	0.1	86.1	17	0.104	0.1	0	4

the dependence of the classical physical model on microstructure, so that it can quickly predict the mechanical properties based on the alloy compositions.

Figures 2(a) and 2(b) describe the influence of the change ratio in (Ni + Co)/Si and Al/(Ti + Zr + V) on the mechanical properties by using composition-UTS model, composition-EL model, and composition-FC model. As a result, the mechanical properties of Cu-Zn alloys are fluctuated with the change ratio in (Ni + Co)/Si and Al/(Ti + Zr + V), agreeing with the general trend from the experiment. Previous experimental studies [25, 26, 27, 28, 29] have shown that the effect of the ratio of (Ni + Co)/Si and Al/(Ti + Zr + V) on the mechanical properties is fluctuating. Since the MLFFANN model relies on the experimental data, the models have the ability to predict in a wide range. Here, the final prediction results show the obvious fluctuations, which are dependent upon the experiment [25, 26, 27, 28, 29]. The increased ratios in (Ni + Co)/Si and Al/(Ti + Zr + V) reduce the value of UTS. The optimum values of (Ni+ Co)/Si and Al/(Ti + Zr + V) are 2 and 3, respectively. For the Cu alloys with the same composition, the EL decreases with increase of UTS. The change trend of EL and UTS appears to be approximately opposite [28, 29, 30]. Figures 2(c)-2(d) depict the influence of the change ratio in (Ni + Co)/Si and Al/(Ti + Zr + V) on FC and the optimum ranges are clearly marked in shadow (UTS × EL is larger, and FC is smaller). The increased ratio in (Ni + Co)/Si and Al/(Ti + Zr + V) reduces the value of FC, and the optimum values of (Ni + Co)/Si and Al/(Ti + Zr + V) are 1.5 and 4, respectively. Thus, the optimum comprehensive mechanical properties of Cu–Zn alloys can be obtained when the ratios (Ni + Co)/Si and Al/(Ti + Zr + V) are 2 and 3. In addition, considering the economic benefit, the ratio should be as the relatively small value.

Many previous studies [27, 28, 29, 30] have analyzed the strengthening mechanism of the Cu–Ni–Si–Co alloy system based on the results of transmission electron microscopy (TEM) and X-ray diffraction (XRD). The strengthening of Cu–Ni–Si–Co alloys with the same structure and the similar lattice parameter is mainly due to the precipitation of Ni₂Si and Co₂Si phases. Further TEM study shows that the precipitated phase structure of the alloy is δ -Ni₂Si in the maximum strengthening range [30, 31, 32, 33]. In fact, the nucleation rate of the Ni₂Si phase is much faster than that of the Co₂Si

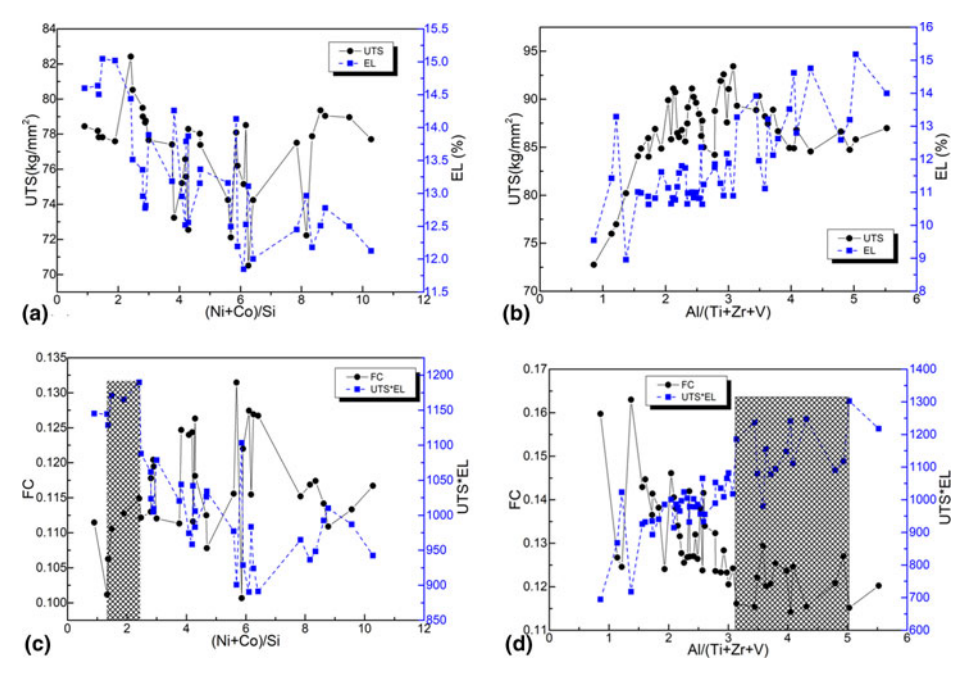


Figure 2: The influence of the change ratio in (a,c) (Ni+Co)/Si and (b,d) AI/(Ti+Zr+V) on the mechanical properties of Cu–Zn alloys.

phase. When the Cu alloy is cast, a large number of Ni₂Si phases nucleate. For refining the grain size, Cu alloys with Ni₂Si phases have excellent tribological properties because Ni₂Si phases have high strengths, high toughness, and strong atomic bonds. After adding Co, the precipitates are similar to the Cu–Ni–Si alloy system and do not increase with the increase of the Co concentration [29, 30, 31, 32, 33].

Furthermore, Al, Ti, Zr, and V can also be added to the Cu alloys to achieve the purpose of precipitation strengthening [33, 34, 35]. The introduction of alloy elements, such as V, Zr, and Ti, which have low diffusivity and solubility, can form thermally stable precipitates. This method is believed to maintain high strengths at temperatures up to 350 °C. These transition elements nucleate and precipitate in the form of Al₃X. The structure of the Al₃X phase is similar to that of Ni₃Al in Ni-based superalloys. It is a kind of trialuminum compound with a cubic L₁₂ structure. It can also keep the coherence with the matrix at high temperatures. Hence, it can enhance the strength of the alloys. However, these precipitates are brittle in nature because they have less slip systems and higher stacking fault energies. At room temperature, trialuminum compounds may lose symmetry with the matrix and have a significant impact on plasticity. Therefore, the strengthening effect of the trialuminum compound may be at the cost of elongation, but high hardness and high strength lead to excellent friction performance. This trend makes up for the defect of plasticity decline [30, 31, 32, 33, 34, 35]. To find the best element proportion of precipitation strengthening, the best proportion predicted by machine learning is close to the proportion of precipitation formed by alloy elements [33, 34, 35]. For example, the proportion of precipitates formed by Ni₂Si or Co₂Si is 2:1, and the optimal proportion predicted by machine learning is also 2. The prediction results of machine learning also have been proved based on the previous work on precipitation strengthening [27, 28, 29, 30, 31, 32, 33, 34, 35]. The atomic ratio of (Ni + Co)/Si should be 2, such as the mass ratio of 4. This way can ensure that all solute atoms are separated from the Cu matrix. Hence, the current findings reveal that machine learning based on different attribute labels can be an efficient and accurate mean for the design of Cu alloy.

Figures 3(a) and 3(c) show the effect of the concentration of the P on the mechanical properties of Cu-Zn alloys. The value of UTS decreases with the increase of the P concentration [33, 34, 35, 36]. The value of UTS reaches the lowest value when the concentration is 0.9, and then shows a rising trend. With the increase of the P concentration, the value of EL firstly shows an upward trend and reaches the maximum value at the concentration of 0.5. Then, it shows a downward trend with the increase of the P concentration. The change trend of the friction coefficient with the change of the P concentration is approximately opposite to the change trend of UTS. As a result, FC reaches the maximum value at the concentration of 1. According to the principle of the best comprehensive properties (UTS × EL is greater, FC is smaller), the best concentration range of the P can be determined and marked by shadow [Fig. 3(c)].

In fact, in the early stage of the P addition, P elements dissolve in Al rapidly, reacting with Al rapidly to form AlP phase, and disperse in the alloy melt. The Al–P phase has a crystal structure, and its lattice constant is similar to that of Si. According to the principle of a similar crystal structure and

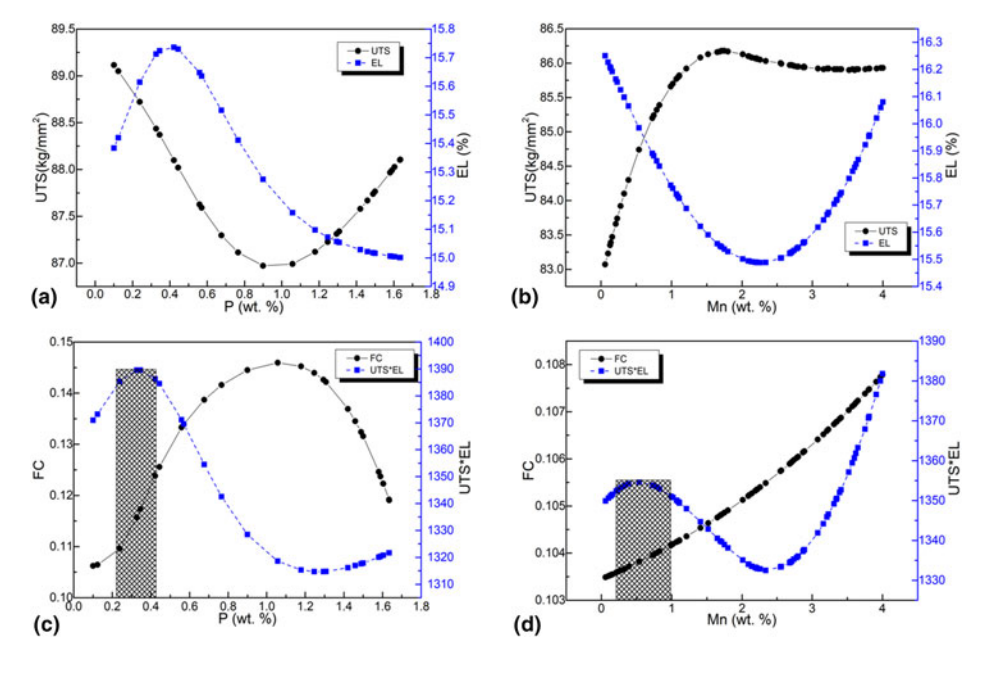


Figure 3: (a,c) The influence of concentration of P on the mechanical properties of Cu–Zn alloys. (b,d) The influence of concentration of Mn on the mechanical properties of Cu–Zn alloys.

🔳 Journal of Materials Research 🔳 Volume 35 🔳 Issue 20 🖿 Oct 28, 2020 📄 www.mrs.org/jmi



Downloaded from https://www.cambridge.org/core. University of Tennessee Libraries, on 01 Jul 2021 at 04:17:48, subject to the Cambridge Core terms of use, available at https://www.cambridge.org/core/terms. https://doi.org/10.1557/jmr.2020.258

lattice constant, Al–P can be used as the heterogeneous nucleus of the Si crystal in the alloy. It makes the Si atom cling to it and crystallize into fine primary Si crystal independently. This fact leads to refining the original coarse Si crystal particles so as to enhance the mechanical properties of the alloy. However, with the increase of P concentration, the P nucleates rapidly in α -Cu matrix, and the vermicular Cu₃P phase is distributed at the grain boundary of α -Cu grain [36, 37, 38, 39]. The Cu₃P phase has high hardness and excellent tribological properties, which can effectively improve the wear resistance of the alloy. However, Cu₃P is brittle, which makes the improvement of wear resistance at the expense of UTS and EL [36, 37, 38]. Therefore, adding P to the Cu alloy requires a specific range to maximize the strengthening effect and minimize the negative effect.

Figures 3(b) and 3(d) show the effect of the concentration of the Mn on the mechanical properties of Cu–Zn alloys. The value of UTS increases with the decrease of the Mn concentration and reaches the maximum value when the concentration is 2. Then, the value of UTS shows a steady trend. With the increase of Mn concentration, the value of EL firstly shows a downward trend and reaches the minimum value at the concentration of 2.2. Then, the value of EL shows a rising trend with the increase of the Mn concentration. In addition, with the decrease of Mn concentration, the value of the FC shows a rising trend and reaches the maximum value at the concentration of 4. Based on the principle of the best comprehensive properties, the optimum concentration range of Mn can be determined, as shown in Fig. 3(d).

Due to the high solubility of Mn in the Cu matrix, the strengthening of Cu alloys is mainly solution strengthening. With the increase of Mn concentration, Mn diffuses continuously in the Cu matrix to form a continuous solid solution. Here, the atomic radii of Cu and Mn are 1.57 and 1.79 Å, respectively. The difference between the atomic radii of Cu and Mn is 14%, leading to the distortion of local crystal lattice and the strain field. At the same time, there is a strain field around the dislocation in the solid solutions. According to the electronic theory of solid solution, the Cu atoms around Mn atoms undergo hetero step transition under the effect of

TABLE 2: The best range of elemental concentration or ratio.

Element	(Ni + Co)/Si	Р	Mn	Al/(Ti + Zr + V)
Lower limits	1.7	0.18	0.3	3.2
Upper limits	2.4	0.38	1	5

the compressive stress and result in more valence electrons [40, 41, 42], because the single-bond half-distance of Mn is larger than that of Cu. In the process of solid solution, Mn can provide more valence electrons. In other word, more covalence electron pairs can be formed between Cu and Mn, resulting in the increase of bond strength in the solid solution. This trend effectively improves the strength and hardness of the Cu alloys. However, when the concentration of Mn is too high, it may lead to the formation of MnO. This trend greatly hinders the diffusion of Mn into the Cu matrix and reduces the strength and hardness [40, 41, 42, 43]. Therefore, the concentration of Mn should be in a suitable range.

The first-best range of elemental concentrations is listed in Table 2, to design the new Cu–Zn alloys. In Table 3, the predicted copper alloy shows the better comprehensive performance compared to the original data set. Due to the limitation of time and resources, the experimental method can not traverse all Cu alloy systems in a wide range at the same processing route. The MLFFANN models can predict the alloy system quickly and accurately. Therefore, the new alloy system proposed in Table 3 is optimal. It can be seen that based on the MLFFANN algorithm, a "composition-oriented" design method for high performance wear-resistant Cu–Zn alloys achieves good results. In the future, to develop the high-performance Cu alloy system, the experimental initial value can be selected from our prediction results from Tables 2 and 3.

Conclusion

The "composition-oriented" method combined with machine learning is used to predict the Cu–Zn alloys with the great strengths, high ductility, and low friction coefficient. The effects of elemental concentrations on the mechanical

TABLE 3: Comparison of the performance of Cu–Zn alloys designed by machine learning with the best comprehensive performance of the original data set of Cu–Zn alloy.

Samples	UTS (kg/mm²)	EL (%)	FC
Cu-29.3Zn-5.5Al-1.74Ti-0.0053Si [21]	83	19	0.11
Cu-29Zn-10Al-1.2Ti-1.2Zr-1.05V-1.6Ni-1Co-0.24P-1.8Si-1Mn	91.3	22.4	0.15
Cu-29Zn-10Al-1.4Ti-1Zr-1.05V-1Ni-1.6Co-0.24P-1.8Si-1Mn	91.9	21.9	0.14
Cu-29Zn-10Al-0.8Ti-1.6Zr-1.05V-0.9Ni-1.7Co-0.24P-1.8Si-1Mn	90.5	22.2	0.14
Cu-29Zn-10Al-0.9Ti-1.5Zr-1.05V-0.7Ni-1.9Co-0.24P-1.8Si-1Mn	90.9	21.9	0.137
Cu-29Zn-10Al-0.9Ti-1.2Zr-1.35V-0.7Ni-1.9Co-0.24P-1.8Si-1Mn	91.3	22	0.128
Cu-29Zn-10Al-0.9Ti-1.1Zr-1.45V-0.8Ni-1.8Co-0.24P-1.8Si-1Mn	91.4	22.2	0.127

TABLE 4: The lower and upper limits of various elements in the original data, where the content of alloy element is weight percent (wt%), and content of O₂ is ppm.

Element	Cu	Zn	Al	02	Ti	Zr	V	Fe	Ni	Со	Р	Mg	Ca	Mn	Sn	Si	Pb
Lower limit	51.56	17.2	2.1	51	0	0	0	0	0	0	0	0	0	0	0	0	0
Upper limit	76.23	39.8	10.9	2980	3.47	3.47	3.42	2.96	2.96	2.94	0.29	0.29	0.27	3.96	2.46	1.33	1.47

TABLE 5: The range of ultimate tensile strength, elongation, and friction coefficient.

Properties	Ultimate tensile strength (kg/mm²)	Elongation (%)	Friction coefficient
Lower limit alloy	69	9.5	0.014
Upper limit alloy	95	20	0.145

properties are analyzed, and the optimal ranges of elemental concentrations are determined. Here, the predicted results of Cu–Zn alloys with the optimal concentrations have better comprehensive mechanical performance. The present work indicates a great potential of the composition-oriented method combined with machine learning to design the advanced materials with high performance.

Methodology

Data preparation

For decades, the development of high-performance Cu alloys has always experienced a surge in popularity, and a lot of data about mechanical properties has been accumulated. The detailed process parameters and relatively rich data from the previous work [22, 44] would be used as the original data set for the machine learning. The data includes the ultimate tensile

strength (UTS), elongation (EL), and friction coefficient (FC), and the corresponding material compositions. Here, a database of 179 well-labeled samples is built for the machine learning. Table 4 lists the upper and lower limits of various elements. Table 5 shows the range of properties of UTS, EL, and FC in the database.

Machine learning

Multi-layer feed-forward artificial neural network (MLFFANN) algorithm [45] is adopted to develop a machine learning model. The construction and efficiency of the MLFFANN model are mainly to determine six parameters, including the number of the hidden layers and neurons, training epochs, activation functions, optimizer, and learning rate. Using the "trial and error" method, these parameters are determined. In addition, the determination of descriptor has a crucial effect on the construction of the MLFFANN model [46]. In the present work, the ratios between different elements, such as (Ni+ Co)/Si, can not be used as the descriptor in training. Elemental ratio neither directly evaluate the effect of a certain element on the property nor adjust directly the composition. The MLFFANN model in the current work is composed of an input layer, two hidden layers, and one output layer (Fig. 4). At the stage of model evaluation (see Fig. 5), under the same optimal parameters of neural network, the

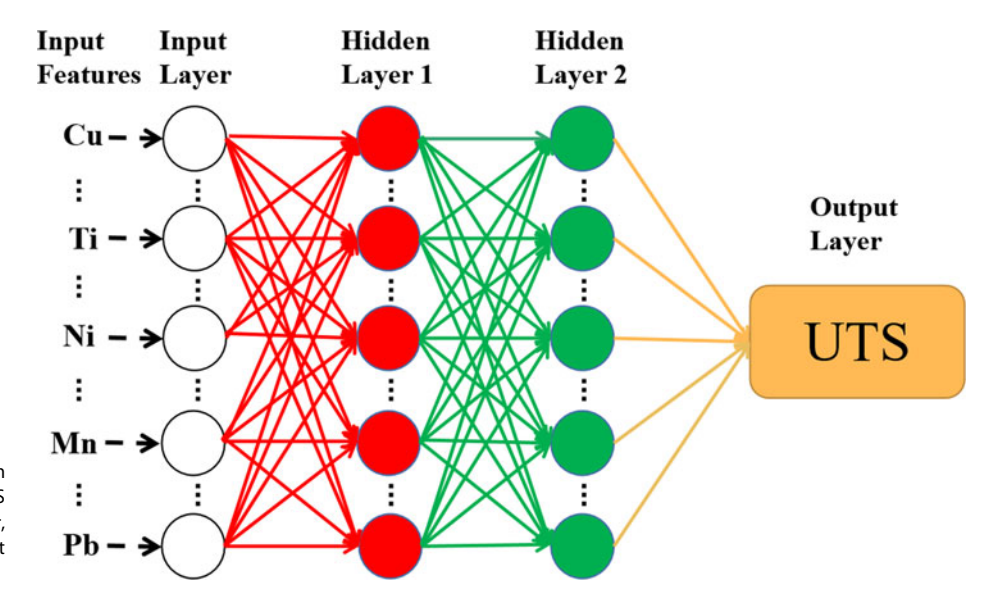


Figure 4: An architecture of an MLFFANN for composition-UTS model, consisting of an input layer, two hidden layers, and one output layer.

🔳 Journal of Materials Research 🔳 Volume 35 🔳 Issue 20 🖿 Oct 28, 2020 📄 www.mrs.org/jmi



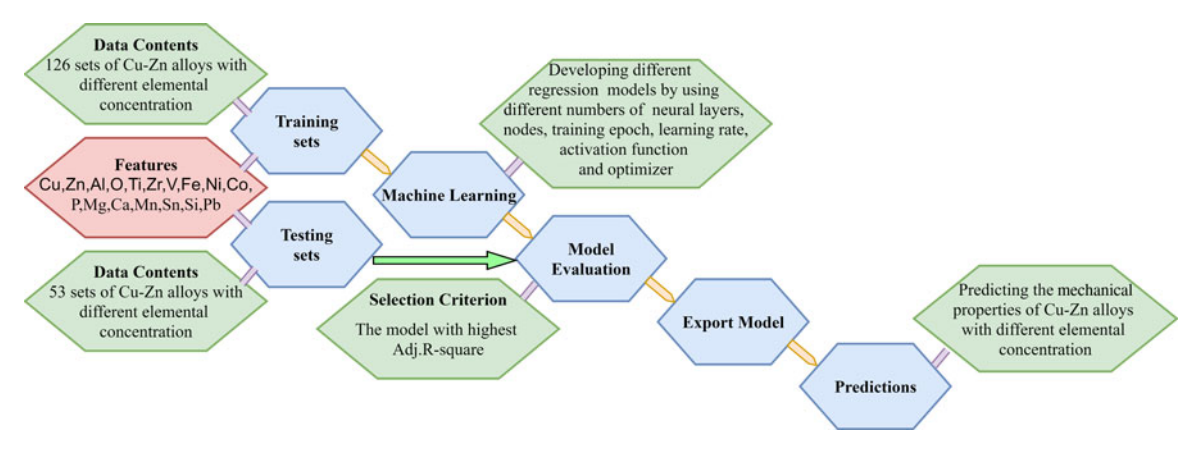


Figure 5: Flowchart for constructing the composition-UTS model, composition-EL model, and composition-FC model.

construction of training set becomes the key factor to affect the accuracy of the MLFFANN model. At present, the common way for constructing the training set is to select a certain number of samples randomly from the original data set [22]. In this work, considering the number of samples in the original data set, we randomly select 100 times in the original data set and calculate the accuracy of these MLFFANN models. The optimal MLFFANN model presents higher accuracy among the 100 random selections.

There are three attribute labels in the original data set; however, the MLFFANN models in the current work can only predict one of them at one time. To this end, the MLFFANN algorithm with the same parameters is used to train three attribute labels separately. Here, three MLFFANN models, including composition-UTS model, composition-EL model, and composition-FC model, are built. The machine-learning design system consists of five major processes (Fig. 5), including building of the data set, machine learning, model evaluation, export model, and prediction.

Here, we need to point out that the predicted result of the MLFFANN model relies heavily on experimental data. The referenced experiments only give the effect of elemental composition on the performance at the same processing conditions. On the other hand, the microstructure is not mentioned in the experiment [22], thus the current MLFFANN model does not consider the effect of microstructure on UTS, EL, and FC.

Acknowledgments

The authors would like to deeply appreciate the support from the Foundation for Innovative Research Groups of the National Natural Science Foundation of China (Grant No. 51621004), the NNSFC (11772122 and 51871092), and the National Key Research and Development Program of China (2016YFB0700300). P.K.L. very much appreciates the supports from (i) the National Science Foundation (DMR-1611180 and

1809640) with program directors, Drs. J. Yang, G. Shiflet, and D. Farkas and (ii) the US Army Research Office (W911NF-13-1-0438 and W911NF-19-2-0049) with program managers, Drs. M.P. Bakas, S.N. Mathaudhu, and D.M. Stepp.

Conflict of interest

The authors declare that they have no conflict of interest.

References

- 1. M. Tang, Y. Zhang, S. Jiang, J. Yu, B. Yan, C. Zhao, and B. Yan: Microstructural evolution and related mechanisms in NiTiCu shape memory alloy subjected local canning compression. Intermetallics 118, 106700 (2020).
- 2. X.H. An, Q.Y. Lin, S.D. Wu, Z.F. Zhang, R.B. Figueiredo, N. Gao, and T.G. Langdon: The influence of stacking fault energy on the mechanical properties of nanostructured Cu and Cu-Al alloys processed by high-pressure torsion. Scr. Mater. 64, 954 (2011).
- 3. Y.H. Zhao, X.Z. Liao, Z. Horita, T.G. Langdon, and Y.T. Zhu: Determining the optimal stacking fault energy for achieving high ductility in ultrafine-grained Cu-Zn alloys. Mater. Sci. Eng. A 493, 123 (2008).
- 4. Y. Jiang, Z. Li, Z. Xiao, Y. Xing, Y. Zhang, and M. Fang: Microstructure and properties of a Cu-Ni-Sn alloy treated by two-stage thermomechanical processing. JOM 71, 2734 (2019).
- 5. B. Luo, D. Li, C. Zhao, Z. Wang, Z. Luo, and W. Zhang: A low Sn content Cu-Ni-Sn alloy with high strength and good ductility. Mater. Sci. Eng. A 746, 154 (2019).
- 6. A. Inoue, W. Zhang, T. Zhang, and K. Kurosaka: High-strength Cu-based bulk glassy alloys in Cu-Zr-Ti and Cu-Hf-Ti ternary systems. Acta Mater. 49, 2645 (2001).
- 7. E. Sjölander and S. Seifeddine: The heat treatment of Al-Si-Cu-Mg casting alloys. J. Mater. Process. Technol. 210, 1249 (2010).



Downloaded from https://www.cambridge.org/core. University of Tennessee Libraries, on 01 Jul 2021 at 04:17:48, subject to the Cambridge Core terms of use, available at https://www.cambridge.org/core/terms. https://doi.org/10.1557/jmr.2020.255

- K.S. Kim, S.H. Huh, and K. Suganuma: Effects of cooling speed on microstructure and tensile properties of Sn–Ag–Cu alloys. *Mater. Sci. Eng. A* 333, 106 (2002).
- D. Tang, L. Wang, J. Li, Z. Wang, C. Kong, and H. Yu: Microstructure, element distribution, and mechanical property of Cu9Ni6Sn alloys by conventional casting and twin-roll casting. *Metall. Mater. Trans. A* 51, 1469 (2020).
- C.B. Basak and A.K. Poswal: Compositional partitioning during the spinodal decomposition in Cu–Ni–Sn alloy. *Philos. Mag.* 98, 1204 (2018).
- G.B. Schaffer, S.H. Huo, J. Drennan, and G.J. Auchterlonie: The effect of trace elements on the sintering of an Al–Zn–Mg–Cu Alloy. *Acta Mater.* 49, 2671 (2001).
- C. Kuehmann and G.B. Olson: Computational materials design and engineering. *Mater. Sci. Eng. A* 25, 472 (2009).
- R.C. Reed, T. Tao, and N. Warnken: Alloys-by-design: Application to nickel-based single crystal superalloys. *Acta Mater*. 57, 5898 (2009).
- 14. G. Kim, H. Diao, C. Lee, A.T. Samaei, T. Phan, M. De Jong, and W. Chen: First-principles and machine learning predictions of elasticity in severely lattice-distorted high-entropy alloys with experimental validation. *Acta Mater.* 181, 124 (2019).
- S. Datta and M.K. Banerjee: Mapping the input-output relationship in HSLA steels through expert neural network. *Mater. Sci. Eng. A* 420, 254 (2006).
- H.K.D.H. Bhadeshia, D.J.C. MacKay, and L.E. Svensson: Impact toughness of C-Mn steel arc welds - Bayesian neural network analysis. *Mater. Sci. Technol.* 11, 1046 (1995).
- J.H. Pak, J.H. Jang, H.K.D.H. Bhadeshia, and L. Karlsson: Optimization of neural network for Charpy toughness of steel welds. *Mater. Manuf. Process.* 24, 16 (2008).
- 18. C.T. Wu, H.T. Chang, C.Y. Wu, S.W. Chen, S.Y. Huang, M.X. Huang, Y.T. Pan, P. Bradbury, J. Chou, and H.W. Yen: Machine learning recommends affordable new Ti alloy with bone-like modulus. *Mater. Today* 34, 41 (2020).
- 19. J. Li, B.B. Xie, Q.H. Fang, B. Liu, Y. Liu, and P.K. Liaw: High-throughput simulation combined machine learning search for optimum elemental composition in medium entropy alloy. *J. Mater. Sci. Technol.* doi: https://doi.org/10.1016/j.jmst.2020.08. 008. Published online 9 August 2020.
- N.S. Reddy, J. Krishnaiah, H.B. Young, and J.S. Lee: Design of medium carbon steels by computational intelligence techniques. *Comput. Mater. Sci.* 101, 120 (2015).
- **21. M.S. Ozerdem and S. Kolukisa**: Artificial neural network approach to predict the mechanical properties of Cu-Sn-Pb-Zn-Ni cast alloys. *Mater. Des.* **30**, 764–769 (2009).
- **22. H. Akutsu and S. Saitama**: Synchronizerring in speed varator made of wear-resistant copper alloy having high strength and toughness. U.S. Patent, 4874439, 1989.

- M. Kuhn: Building predictive models in R using the caret package.
 J. Stat. Softw. 28, 1–26 (2008).
- 24. J. Li, L. Li, C. Jiang, Q. Fang, F. Liu, Y. Liu, and P.K. Liaw: Probing deformation mechanisms of gradient nanostructured CrCoNi medium entropy alloy. J. Mater. Sci. Technol. 57, 85–91 (2020).
- 25. L. Li, H. Chen, Q. Fang, J. Li, F. Liu, Y. Liu, and P.K. Liaw: Effects of temperature and strain rate on plastic deformation mechanisms of nanocrystalline high-entropy alloys. *Intermetallics* 120, 106741 (2020).
- 26. Y. Zhang, S. Jin, P.W. Trimby, X. Liao, M.Y. Murashkin, R.Z. Valiev, J. Liu, J.M. Cairney, S.P. Ringer, and G. Sha: Dynamic precipitation, segregation and strengthening of an Al-Zn-Mg-Cu alloy (AA7075) processed by high-pressure torsion. Acta Mater. 162, 19–32 (2019).
- 27. J.Y. He, H. Wang, H.L. Huang, X.D. Xu, M.W. Chen, Y. Wu, X.J. Liu, T.G. Nieh, K. An, and Z.P. Lu: A precipitation-hardened high-entropy alloy with outstanding tensile properties. *Acta Mater*. 102, 187–196 (2016).
- 28. Y.H. Gao, L.F. Cao, C. Yang, J.Y. Zhang, G. Liu, and J. Sun: Co-stabilization of θ'-Al₂Cu and Al₃Sc precipitates in Sc-microalloyed Al-Cu alloy with enhanced creep resistance. *Mater. Today* 6, 100035 (2019).
- 29. J. Yi, Y.L. Jia, Y.Y. Zhao, Z. Xiao, K.J. He, Q. Wang, M.P. Wang, and Z. Li: Precipitation behavior of Cu-3.0Ni-0.72Si alloy. *Acta Mater.* 166, 261–270 (2019).
- 30. H.M. Wen, T.D. Topping, D. Isheim, D.N. Seidman, and E.J. Lavernia: Strengthening mechanisms in a high-strength bulk nanostructured Cu-Zn-Al alloy processed via cryomilling and spark plasma sintering. Acta Mater. 61, 2769–2782 (2013).
- Q. Lei, Z. Li, T. Xiao, Y. Pang, Z.Q. Xiang, W.T. Qiu, and
 Z. Xiao: A new ultrahigh strength Cu-Ni-Si alloys. *Intermetallics* 42, 77–84 (2013).
- **32.** H.A. Elhadari, H.A. Patel, D.L. Chen, and W. Kasprzak: Tensile and fatigue properties of a cast aluminum alloy with Ti, Zr and V additions. *Mater. Sci. Eng. A* **528**, 8128–8138 (2011).
- 33. T. Hu, J.H. Chen, J.Z. Liu, Z.R. Liu, and C.L. Wu: The crystal-lographic and morphological evolution of the strengthening precipitates in Cu-Ni-Si alloys. *Acta Mater.* 61, 1210–1219 (2013).
- 34. J. Li, G.J. Huang, X.J. Mi, L.J. Peng, H.F. Xie, and Y.L. Kang: Effect of Ni/Si mass ratio and thermomechanical treatment on the microstructure and properties of Cu-Ni-Si alloys. *Materials* 12, 2076 (2019).
- H. Turhana, M. Aksoyb, V. Kuzucuc, and M.M. Yildirim: The effect of manganese on the microstructure and mechanical properties of leaded-tin bronze. *J. Mater. Process. Technol.* 114, 207– 211 (2001).
- H. Men, W.T. Kim, and D.H. Kim: Effect of titanium on glassforming ability of Cu-Zr-Al alloys. *Mater. Trans.* 44, 1647–1650 (2003).



- 37. M. Aksoy, V. Kuzucu, and H. Turhan: A note on the effect of phosphorus on the microstructure and mechanical properties of leaded-tin bronze. J. Mater. Process. Technol. 124, 113-119 (2002).
- 38. X. Ma, J. Chen, Y. Liu, X. Wang, and S. Huang: Effect of shortrange order on microstructure, texture and strain hardening of cold drawn Cu-10at.%Mn alloy. Mater. Charact. 135, 32-39 (2018).
- 39. L. Liu, Z. Chen, C. Liu, Y. Wu, and B. An: Micro-mechanical and fracture characteristics of Cu₆Sn₅ and Cu₃Sn intermetallic compounds under micro-chatilever bending. Intermetallics 76, 10 (2016).
- 40. R. Sandstrom and H. Andersson: The effect of phosphorus on creep in copper. J. Nucl. Mater. 372, 66 (2008).
- 41. S.M. Dar, H.C. Liao, and A. Xu: Effect of Cu and Mn content on solidification microstructure, T-phase formation and mechanical property of Al-Cu-Mn alloys. J. Alloys Compd. 774, 758 (2019).
- 42. X.H. An, S.D. Wu, Z.G. Wang, and Z.F. Zhang: Significance of stacking fault energy in bulk nanostructured materials: insights

- from Cu and its binary alloys as model systems. Prog. Mater. Sci. **101**, 1 (2019).
- 43. Y.Z. Tian, L.J. Zhao, N. Park, R. Liu, P. Zhang, Z.J. Zhang, A. Shibata, Z.F. Zhang, and N. Tsuji: Revealing the deformation mechanisms of Cu-Al alloys with high strength and good ductility. Acta Mater. 110, 61 (2016).
- 44. S.C. Krishna and J. Srinath: Microstructure and properties of a high-strength Cu-Ni-Si-Co-Zr alloy. J. Mater. Eng. Perform. 22, 2115 (2013).
- 45. L.O. Orimoloye, M.C. Sung, T. Ma, and J.E.V. Johnson: Comparing the effectiveness of deep feedforward neural networks and shallow architectures for predicting stock price indices. Expert Syst. Appl. 139, 112828 (2020).
- 46. V. Nourani, H. Gökçekuş, and I.K. Umar: Artificial intelligence based ensemble model for prediction of vehicular traffic noise. Environ. Res. 180, 108852 (2020).